



Synthesis, characterization, biological activities, crystal structure and DNA binding of organotin(IV) 5-chlorosalicylates

Shabbir Hussain, Saqib Ali, Saira Shahzadi, Muhammad Nawaz Tahir & Muhammad Shahid

To cite this article: Shabbir Hussain, Saqib Ali, Saira Shahzadi, Muhammad Nawaz Tahir & Muhammad Shahid (2015) Synthesis, characterization, biological activities, crystal structure and DNA binding of organotin(IV) 5-chlorosalicylates, Journal of Coordination Chemistry, 68:14, 2369-2387, DOI: [10.1080/00958972.2015.1046849](https://doi.org/10.1080/00958972.2015.1046849)

To link to this article: <http://dx.doi.org/10.1080/00958972.2015.1046849>



Accepted author version posted online: 05 May 2015.
Published online: 27 May 2015.



Submit your article to this journal [↗](#)



Article views: 99



View related articles [↗](#)



View Crossmark data [↗](#)



Citing articles: 2 View citing articles [↗](#)

Synthesis, characterization, biological activities, crystal structure and DNA binding of organotin(IV) 5-chlorosalicylates

SHABBIR HUSSAIN[†], SAQIB ALI^{*‡}, SAIRA SHAHZADI^{*‡}, MUHAMMAD NAWAZ TAHIR[§] and MUHAMMAD SHAHID[¶]

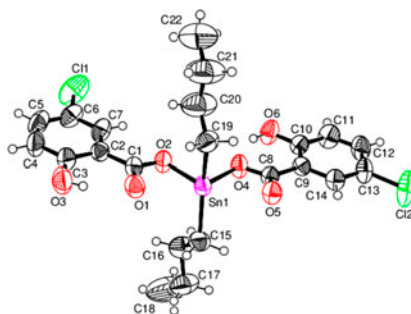
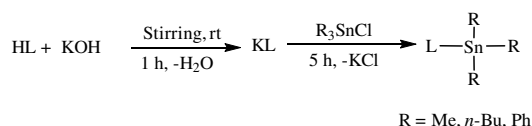
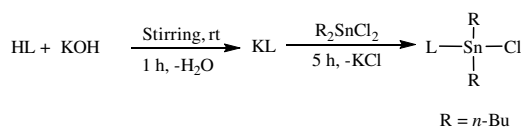
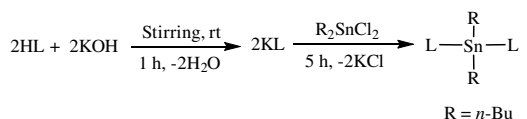
[†]Department of Chemistry, GC University, Faisalabad, Pakistan

[‡]Department of Chemistry, Quaid-i-Azam University, Islamabad, Pakistan

[§]Department of Physics, University of Sargodha, Sargodha, Pakistan

[¶]Department of Chemistry and Biochemistry, University of Agriculture, Faisalabad, Pakistan

(Received 27 October 2014; accepted 9 April 2015)



*Corresponding authors. Email: drsa54@yahoo.com (S. Ali); sairashahzadi@hotmail.com (S. Shahzadi)

New organotin(IV) carboxylates, R_2SnL_2 ($R=n$ -Bu: **1**), $R_2Sn(Cl)L$ ($R=n$ -Bu: **2**), and R_3SnL ($R=Me$: **3**; n -Bu: **4**; Ph: **5**) have been synthesized by stirring 5-chloro-2-hydroxybenzoic acid **HL** with KOH and R_2SnCl_2 ($R=n$ -Bu)/ R_3SnCl ($R=Me$, n -Bu, Ph) in methanol at room temperature. The complexes along with ligand have been characterized by FTIR, (1H , ^{13}C) NMR, EI-MS, and single-crystal XRD crystallography. FTIR data indicated bidentate coordination of carboxylate. NMR data suggested six- or five-coordinate geometry of organotin(IV) carboxylates. Single-crystal XRD of **1** demonstrated skew-trapezoidal geometry around the tin center, with the basal plane occupied by four oxygens and the two butyl groups lying in distorted axial position. Complexes **1**, **2**, and **5** exhibited interaction with SS-DNA (salmon sperm) and suggests intercalating mode of binding. The complexes displayed significant antimicrobial activities against bacterial and fungal strains as compared to free ligand. The hemolytic activity of the complexes was lower compared to Triton-X 100 (positive control, 100% lysis) and higher than phosphate-buffered saline (negative control, 0% lysis). Complex **4** was the most potent inhibitor of bacterial/fungal growth.

Keywords: 5-Chlorosalicylic acid; Organotin(IV); IR; NMR; Mass; XRD; DNA interaction; Biological activities

1. Introduction

The synthetic chemistry of organotin(IV) complexes is a subject of investigation due to their biological and industrial applications. Such compounds have been developed as important thermal stabilizers for plastics, as catalysts, and as biocides [1]. Organotin(IV) carboxylates find applications as catalysts in esterification [2], silicone curing [3], formation of polyurethane [4], antifouling paints [5], PVC stabilization [6], and transesterification of vegetable oil into biodiesel [7]. They also have been applied as anti-bacterial and anti-fungal agents and have received considerable attention as anti-tumor and anti-cancer drugs [8] due to their ability to bind with phosphate of DNA in tumor cells and damage it. Their biological activity is usually associated with organotin(IV) moieties [9] and the organic ligand [10], since the organic ligand facilitates the transportation of the complexes across the cell membrane. In general, triorganotin compounds display higher biological activity than their di- and monoorganotin analogs, attributed to their ability to bind proteins [11]. Organotin(IV) complexes have structural diversity including differences in coordination number and molecular geometry [12], as they have a large number of structure types, including monomers, dimers, tetramers, oligomeric ladders, hexameric drums [13], and polymeric 3-D crystal lattice [14].

In continuation of our previous work on organotin complexes [14–16], we report here the synthesis and characterization of organotin(IV) carboxylates with 5-chloro-2-hydroxybenzoic acid. Different structural types are formed due to the presence of additional coordinating sites along with a carboxylate moiety. Thus, it appears that the preference of a particular tin carboxylate to adopt a given structure stems from a combination of steric and electronic factors [17]. The synthesized complexes have been characterized by IR, NMR (1H and ^{13}C), EI-MS, and single-crystal XRD. The organotin(IV) carboxylates were also tested for their anti-bacterial and anti-fungal activities. DNA interaction studies and *in vitro* hemolytic bioassays of complexes were also performed.

2. Experimental

2.1. Materials and methods

Dibutyltin dichloride, trimethyltin chloride, tributyltin chloride, and triphenyltin chloride were purchased from Sigma-Aldrich (USA) and used without purification.

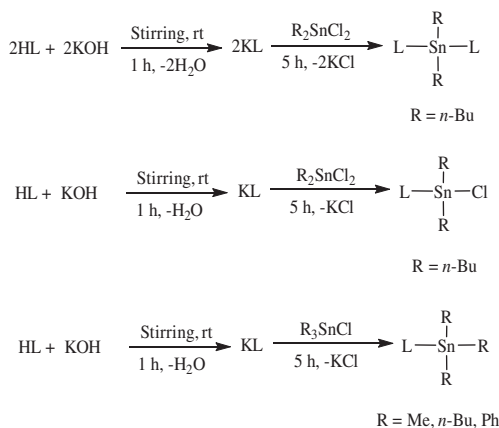
5-Chloro-2-hydroxybenzoic acid **HL** was purchased from Merck (Germany). AR grade solvents of Merck (methanol, chloroform), Lab-scan (DMSO), and Riedel-de Haen (petroleum ether) were used. The solvents were dried before use by standard procedures [18].

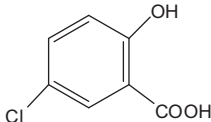
The samples were taken in capillary tubes and their melting points were recorded by an electrochemical melting point apparatus Stuart SMP3 and are uncorrected. Infrared spectra were recorded by a Perkin–Elmer-1000 FTIR spectrophotometer from 4000 to 250 cm^{-1} . The percentage composition of C and H was determined using a CHNS-932 elemental analyzer, Leco (USA). The ^1H and ^{13}C NMR spectral measurements were made at 300 and 75 MHz, respectively, by a Bruker ARC 300 MHz-FT-NMR spectrometer. EI mass spectra were recorded using a Thermo Fisher Exactive Orbitrap instrument. The X-ray diffraction data were collected on a Bruker SMART APEX CCD diffractometer equipped with a 4 K CCD detector set 60.0 mm from the crystal. The crystals were cooled using a Bruker KRYOFLEX low temperature device at 100 ± 1 K, and intensity measurements were carried out from a sealed ceramic diffraction tube (SIEMENS) using graphite monochromated $\text{Mo K}\alpha$ radiation. Generator settings were 50 kV/40 mA. The structure was solved by the Patterson method, and extension of the model was accomplished by direct method using the program DIRDIF or SIR2004. Final refinement on F^2 carried out by full matrix least squares techniques using SHELXL-97, a modified version of the program PLUTO and PLATON package.

The complexes were tested for their interaction with salmon sperm DNA (SS-DNA) [19, 20]. Antimicrobial activities of the ligand and the complexes were tested against bacteria (*Escherichia coli*, *Bacillus subtilis*, *Staphylococcus aureus*, and *Pasturella multocida*) and fungi (*Alternaria alternata*, *Ganoderma lucidum*, *Penicillium notatum*, *Trichoderma harzianum*, and *Aspergillus niger*) by the disk diffusion method [21, 22] and minimum inhibitory concentration (MIC) [23]. The activities were performed in an incubator (Sanyo, Germany) and sterilized in an autoclave (Omron, Japan). The MIC was determined in a Micro Quant apparatus (BioTek, USA). Streptomycin and fluconazole were used as standard drugs for antibacterial and antifungal activities, respectively. The *in vitro* hemolytic bioassay [24] of the complexes was reported with respect to the Triton-X 100 as positive control and phosphate-buffered saline (PBS) as negative control.

2.2. General procedure for synthesis of 1–5

5-Chloro-2-hydroxybenzoic acid **HL** (2/1 mmol) and KOH (2/1 mmol) were stirred together in methanol (50 mL) for 1 h in a round bottom flask (100 mL) at room temperature. Then, $\text{R}_2\text{SnCl}_2/\text{R}_3\text{SnCl}$ (1 mmol) was added in portions as solid and the reaction mixture was continuously stirred for 5 h. The precipitated KCl was filtered off and solvent was evaporated using a rotary evaporator under reduced pressure. The solid product obtained was recrystallized from methanol and petroleum ether (2:1).



HL	R	Complex number
	<i>n</i> -Bu	1
	<i>n</i> -Bu	2
	Me	3
	<i>n</i> -Bu	4
	Ph	5

2.3. DNA interaction study

The interaction of organotin(IV) complexes with SS-DNA was studied by absorption spectroscopy. A solution of SS-DNA in tris-HCl buffer [5 mM tris(hydroxyl methyl)amino-methane and 50 mM NaCl, pH 7.2] was prepared and gave an absorbance ratio of 1.9 : 1 at 260 and 280 nm, which demonstrated that DNA was free from protein [19, 20]. The DNA concentration was measured at 260 nm using the molar absorption coefficient of $6600 \text{ M}^{-1} \text{ cm}^{-1}$ and was found out to be $7.45 \times 10^{-5} \text{ M}$ [20]. A 2 mM solution of each complex was prepared in 90% DMSO. For UV-Visible absorption titrations, working solutions (2 mL) of a test compound and SS-DNA in 90% DMSO were prepared; these solutions have the same concentration (2 mM) of complex but have different concentrations (10, 19, 27, 35, 42, 48, 54, 59, 64, and 69 μM) of SS-DNA. An equivalent volume of a solution containing the SS-DNA and solvent but lacking the test compound was used as a reference standard to eliminate the absorbance of DNA itself. The solutions were incubated at ambient temperature for 30 min before performing the measurements. Absorption spectra were recorded using cuvettes of 1 cm path length.

2.4. Antimicrobial activities

2.4.1. Growth medium, culture, and inoculum preparation. The bacterial strains (*E. coli*, *B. subtilis*, *S. aureus*, and *P. multocida*) were cultured in nutrient agar (Oxoid, Hampshire, UK) medium at 37 °C overnight. These pure cultures were then maintained in

the same medium in petri plates. For inoculum preparation, 13 g of nutrient broth was added to one liter of distilled water, mixed homogeneously, and was autoclaved for 15 min at 121 °C. To freshly prepared nutrient broth medium (100 mL), a 10 µL pure culture of a bacterial strain was added and the mixture was incubated in a shaker (140 rpm) at 37 °C for 24 h. The prepared inocula were stored at 4 °C in a refrigerator. The inocula with 1×10^8 spores mL⁻¹ were used for further analysis.

The fungal strains (*A. alternata*, *G. lucidum*, *P. notatum*, *T. harzianum*, and *A. niger*) were cultured in potato dextrose agar (Oxoid) medium overnight at 28 °C and the pure cultures were then maintained in the same medium in petri plates which were presterilized in a hot air oven at 180 °C for 3 h. These cultures were incubated at 28 °C for multiplication of fungal strains for 3–4 days.

2.4.2. Antimicrobial assay by disk diffusion method. Antibacterial and antifungal activities of the ligand and complexes were determined by the disk diffusion method [21]. A total of 2.8 g nutrient agar (for antibacterial activities) or 3.9 g of potato dextrose agar (for antifungal activities) was suspended in 100 mL distilled water, and the mixture was sterilized by autoclaving at 121 °C for 15 min. It was then mixed well with 100 µL inoculum of a microbial strain and transferred into sterilized petri plates. Later, small filter paper disks (size, 9 mm), each soaked with 100 µL solution (concentration = 1 mg mL⁻¹ in DMSO) of a test sample, were placed flat on the growth medium. The petri plates were then incubated for 24 h at 37 °C for bacterial growth and for 48 h at 28 °C for fungal growth. The biologically active samples inhibited the bacterial/fungal growth to form clear zones which were measured in millimeters by a zone reader [22].

2.4.3. Antimicrobial assay by minimum inhibitory concentration. The complexes as well as the ligand were evaluated for their MICs by a reported method [23] with some modifications. Plates were prepared under aseptic conditions and carefully labeled. Then, 100 µL solution (concentration = 1 mg mL⁻¹ in DMSO) of each sample was pipetted separately into the first row of a 96-well plate. To the wells of all other rows, 50 µL of nutrient broth medium was added. A multichannel pipette was used for serial dilutions in such a way that each well had 50 µL test material in serially descending concentrations. Later, a 270 mg tablet of resazurin was dissolved in 40 mL of sterile distilled water and 20 µL of this solution was added to each well as an indicator. Finally, 10 µL of bacterial suspension was added to every well and the plate was loosely wrapped with aluminum foil to prevent dehydration of bacteria. Each plate contained a set of controls: a column having all the solutions except the bacterial solution because 10 µL of nutrient broth was added instead, a column with all solutions except the test compound and a column with a broad-spectrum antibiotic, streptomycin, as a positive control. These plates were prepared in triplicate and placed in an incubator for 18–24 h at 37 °C. Afterward, the color changes in each row were assessed visually. The color changes from purple to colorless or pink indicated bacterial growth. The lowest concentration of a compound, at which the color change was observed, was taken as MIC value against a bacterial strain.

MIC values against the fungal strains were measured by adopting the same methodology with the exception that sabouraud dextrose agar medium was used; furthermore, the resazurin indicator was not involved in the procedure. The activities depend on the concentration of the complexes.

2.5. Hemolytic activities

Three milliliter of heparinized human blood was freshly obtained from volunteers after consent. Then, it was mixed gently, transferred into a 15-mL sterile polystyrene screw-cap tube, and centrifuged for 5 min at 850 g. The resultant supernatant mass was poured off and the viscous pellet was washed 3 times with 5 mL of chilled (4 °C) and sterile isotonic PBS of pH 7.4. The washed cells were suspended in 20 mL sterile chilled PBS and counted on a hemacytometer. The blood cell suspension retained on wet ice was diluted for each assay with sterile PBS to 7.068×10^8 cells mL^{-1} . Aliquots of 20 μL of each sample solution were placed aseptically into 2.0 mL microfuge tubes. For each assay, 0.1% Triton-X 100 was used as a positive control (100% lysis) and PBS as a negative control (0% lysis). Aliquot of 180 μL diluted blood cell suspension was aseptically placed into each 2 mL tube and gently mixed with a wide mouth pipette tip three times. The tubes were incubated with agitation (80 revolutions per minute) at 37 °C for 35 min and then placed for 5 min on ice followed by centrifugation at 1310 g for 5 min. Aliquots of 100 μL of supernatant were collected, placed into a sterile 1.5 mL microfuge tube, and then diluted with 900 μL chilled and sterile PBS. All the tubes were maintained on wet ice after dilution. Absorbances were then noted on a microquant at 576 nm. The experiment was performed in triplicate. Percentage hemolysis was calculated by following formula [24]:

$$\% \text{ Hemolysis} = \text{Abs}(\text{sample absorbance}) / \text{Abs}(\text{control absorbance}) \times 100$$

3. Results and discussion

The complexes are stable in air, have sharp melting points, and are soluble in common organic solvents. The physical data are summarized in table 1.

3.1. IR spectroscopy

Infrared spectra of the organotin(IV) carboxylates provide valuable information regarding the structure of compounds and coordination geometry of the metal in the solid state. Infra-red spectra were recorded from 4000 to 250 cm^{-1} . The data are given in table 2. IR spectra of the complexes lack νOH (a broad band) at 3497 cm^{-1} of the carboxylic acid group of

Table 1. Physical data of 1–5.

Complex number	Molecular formula	Mol. wt.	Yield (%)	m.p. (°C)	Elemental analysis calculated (found)	
					%C	%H
HL	$\text{C}_7\text{H}_5\text{O}_3\text{Cl}$	172.57	–	171–172	–	–
1	$\text{C}_{22}\text{H}_{26}\text{O}_6\text{SnCl}_2$	576.02	95	131–132	45.87(45.82)	4.55(4.51)
2	$\text{C}_{15}\text{H}_{22}\text{O}_3\text{SnCl}_2$	439.93	92	111–112	40.95(40.92)	5.04(5.08)
3	$\text{C}_{10}\text{H}_{13}\text{O}_3\text{SnCl}$	335.35	91	94–95	35.82(35.86)	3.91(3.87)
4	$\text{C}_{19}\text{H}_{31}\text{O}_3\text{SnCl}$	461.60	97	122–123	49.44(49.49)	6.77(6.73)
5	$\text{C}_{25}\text{H}_{19}\text{O}_3\text{SnCl}$	521.57	94	129–130	57.57(57.52)	3.67(3.71)

Table 2. IR data^a (cm⁻¹) of **1–5**.

Complex number	νOH carboxylic	νOH phenolic	νCOO		$\Delta\nu$	$\nu\text{Sn-C}$	$\nu\text{Sn-O}$
			Asym	Sym			
HL	3497b	3728b	1686s	1327w	359	–	–
1	–	3751b	1558s	1444s	114	557w	421w
2	–	3716b	1558s	1450s	108	563b	461w
3	–	3736b	1605s	1454s	151	548s	433w
4	–	3740b	1560s	1449s	111	563m	457w
5	–	3687b	1568s	1458s	110	263s	449s

^aAbbreviations: s = strong; m = medium; w = weak; b = broad.

the free ligand due to its deprotonation for coordination with metal. IR spectroscopy demonstrated that phenolic oxygen of the ligand could not develop coordination with Sn (IV) as the $\nu\text{OH}_{(\text{phenolic})}$ stretch (3728 cm⁻¹) of the free ligand was also displayed in the complexes at 3687–3751 cm⁻¹; the non-involvement of phenolic oxygen for coordination with metal was further verified by ¹H NMR and XRD crystallography. The appearance of $\nu\text{OH}_{(\text{phenolic})}$ vibrations as broadbands at 3687–3751 cm⁻¹ demonstrated the presence of intra-molecular hydrogen bonding in the organotin(IV) complexes, which is also verified through single-crystal XRD data of **1** (figure 1).

Such hydrogen bonding actually happens between ortho hydroxyl proton and carbonyl oxygen of tin bonded COO⁻ moiety as also documented by earlier reports [25] regarding organotin(IV) salicylates. The carbonyl stretching frequency of the free ligand shifted to lower wavenumber in complexes, ascribed to metal carboxylate coordination in accordance with earlier reports [26]. The mode of tin carboxylate interaction was predicted from $\Delta\nu = \nu\text{COO}_{(\text{asym})} - \nu\text{COO}_{(\text{sym})}$ value; $\Delta\nu$ lying in the range of 108–151 cm⁻¹ in the complexes suggested bidentate chelating coordination of the carboxylate [26]. Thus, six- and five-coordinate geometries around Sn(IV) were suggested in the solid state for the investigated diorganotin and chlorodiorganotin/triorganotin derivatives, respectively, of 4-chlorosalicylic acid. Similar studies on triphenyltin esters of salicylic acid demonstrated that there is a structural distortion from the tetrahedron toward a trigonal bipyramid [27].

New bands at 548–563 cm⁻¹ (**1–4**) and 263 cm⁻¹ (triphenyltin derivative; **5**) were attributed to Sn–C bond [28] and the Sn–O vibrational frequencies from 421 to 461 cm⁻¹ in **1–5**.

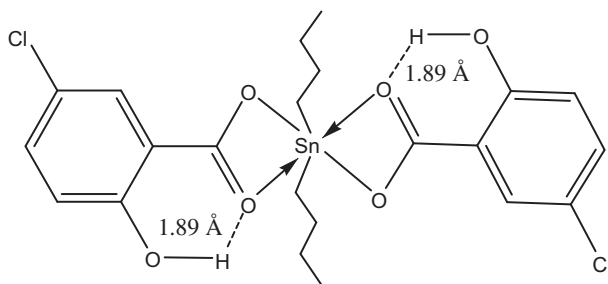
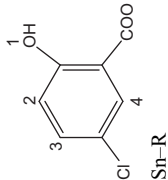


Figure 1. Molecular structure of **1**. The dotted lines show hydrogen bonding.

Table 3. ¹H NMR data^{a,b} of 1–5.

Proton no.	Chemical shift (ppm)					
	HL	1	2	3	4	5
	11.82s	11.82s	11.84s	11.83s	11.84s	11.85s
2	6.97d(8.8)	6.85d(8.7)	6.87d(8.7)	6.83d(8.7)	6.82d(8.7)	6.88d(8.8)
3	7.51d(8.9)	7.35d(8.4)	7.38d(8.4)	7.34d(8.7)	7.39d(8.8)	7.38d(8.7)
4	7.71s	7.70s	7.70s	7.73s	7.72s	7.71s
α	–	1.22–1.33 m	1.22–1.34 m	0.54s[71]	1.15–1.19 m	–
β	–	1.55–1.64 m	1.65–1.66 m	–	1.56–1.66 m	6.69–6.92 m
γ	–	1.55–1.64 m	1.56–1.61 m	–	1.24–1.36 m	6.80–7.30 m
δ	–	0.81t(7.2)	0.83t(7.2)	–	0.85t(7.2)	–

^aMultiplicity is given as: s = singlet, d = doublet, t = triplet, m = multiplet.

^bCoupling constant, ^aJ(¹H, ¹H) and ^aJ(¹H, ¹H) in Hz are given in square brackets and parenthesis, respectively.

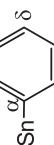


Table 4. (C–Sn–C) angles (°) based on ^1H and ^{13}C NMR parameters.

Complex number	$^1J[^{119}\text{Sn}, ^{13}\text{C}]$ (Hz)	$^2J[^{119}\text{Sn}, ^1\text{H}]$ (Hz)	Angle (°)	
			θ (1J)	θ (2J)
2	147	–	92	–
3	522	71	122	118
4	478	–	123	–

3.2. ^1H NMR spectroscopy

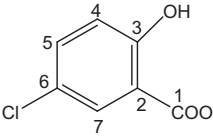
The signals were assigned by their distinct multiplicity patterns, resonance intensities, coupling constants, and tin satellites. The ^1H NMR data are given in table 3. The resonance for carboxylic (–COOH) proton of **HL** disappeared in spectra of complexes indicating deprotonated carboxylate anion. In the complexes, the persistence of ^1H NMR signal for phenolic proton of free **HL** demonstrated its non-involvement in coordination with metal, thus supporting the IR findings. The trimethyltin 5-chlorosalicylate (**3**) exhibited a singlet at 0.54 ppm with $^2J[^{119}\text{Sn}, ^1\text{H}]$ coupling constant of 71 Hz. table 4 represents the coupling constants (nJ) obtained from resolved satellites and the calculated C–Sn–C bond angles (θ) [29] in solution state. The data strongly support five-coordinate geometry (trigonal bipyramidal) around tin in trimethyltin(IV) derivative **3**. The $^2J[^{119}\text{Sn}, ^1\text{H}]$ value (71 Hz) for **3** was considerably higher compared to that observed (57.10 Hz) for a simple trimethyltin salicylate having no chloro-substituent [25]. These observations thus demonstrate an increase in coordination number at tin(IV) due to bonding with a 4-chlorosalicylate ion. A similar five-coordinate (trigonal bipyramidal geometry) environment around Sn(IV) in the solid state was also depicted during X-ray crystallographic analyses of triphenyltin derivatives of *o*- or *p*-chlorobenzoic acids [30].

In **1**, **2**, and **4**, the protons of butyl appear as multiplets at 1.22–1.34 and 1.55–1.66 ppm. Despite the complex pattern of *n*-butyl fragments in **1**, **2**, and **4**, a clear triplet due to terminal methyl group appeared in the range 0.81–0.85 ppm with $^3J(^1\text{H}, ^1\text{H}) = 7.2$ Hz. In triphenyltin(IV) derivative, the phenyl protons consisted of two groups of peaks. Ortho protons absorbed downfield (6.80–7.30 ppm) when compared to meta and para protons (6.69–6.92 ppm) in the phenyltin(IV) derivative **5** [15].

3.3. ^{13}C NMR spectroscopy

The ^{13}C NMR data are given in table 5. The spectra displayed the expected carbon signals of the ligand as well as coordinated Sn–R. The resonance at 171.1 ppm for carboxylate carbon of free ligand shifted downfield to 173.3–174.5 ppm in **1–5** verifying COO–Sn coordination. These chemical shifts (173.3–174.5) are consistent with that ($\delta_{\text{COO}} = 175.1$) reported for trimethyltin salicylate [25]. However, the smaller differences between early reported [25] and investigated δ_{COO} values were rendered to the electron-donating effect of a chloro-substituent which increases the electron density at the aromatic ring. There was a significant downfield shift of carbon labeled as 2 from 114.9 ppm in **HL** to 115.1–115.8 ppm in **1–5**, indicating the flow of electronic charge density from aromatic nucleus toward carboxylic moiety, enabling bidentate coordination of carboxylate with tin(IV).

Table 5. ^{13}C NMR data^a of **1–5**.

	Carbon no.	Chemical shift (ppm)					
		HL	1	2	3	4	5
	1	171.1	173.3	174.4	173.7	174.0	174.5
	2	114.9	115.3	115.1	115.8	115.6	115.7
	3	160.2	160.7	160.5	160.4	160.3	160.1
	4	119.6	119.3	119.3	119.8	119.1	119.7
	5	135.6	133.7	134.0	133.6	133.4	134.7
	6	123.0	122.7	122.0	122.8	122.9	123.0
	7	129.6	129.9	129.4	129.8	129.9	129.6
Sn–R	α	–	26.1	26.0[147]	–2.0[522]	19.8[478]	135.7
	β	–	27.6	27.8[45]	–	28.2[28]	129.6
	γ	–	27.0	27.0	–	26.9[75]	119.7
	δ	–	14.1	14.1	–	14.0	123.0

^aChemical shifts (δ) in ppm: ⁿ $J[^{119}\text{Sn}, ^{13}\text{C}]$ in Hz is listed in square brackets.

The trimethyltin(IV) moiety exhibited a chemical shift at -2.0 ppm in **3**, while the terminal carbon (labeled as δ) of butyl groups in **1**, **2**, and **4** showed resonance at 14.0 – 14.1 ppm. The value of $^1J[^{119}\text{Sn}, ^{13}\text{C}]$ may be used as an indicator of the coordination number of tin in triorganotin compounds (table 4). The trimethyltin(IV) and tributyltin(IV) carboxylates (**3** and **4**) exhibited five-coordinate geometries [29, 31] around Sn(IV). The geometry around tin for diorganotin dicarboxylates (complex **1**) in solution could not be determined with certainty due to fluxional behavior of the carboxylate; however, earlier reports suggest geometry between five- and six-coordinate in such complexes [32].

3.4. Mass spectrometry

The mass spectra were recorded for **HL** and **1–3**. The mass fragmentation data are given in table 6. Each stannic ion appeared in the spectrum as a series of peaks close to each other due to isotopic effects [33].

The mass spectroscopic data agreed well with the molecular skeleton of the ligand and the complexes. Free **HL** showed the molecular ion peak at $m/z = 172$ (54%) followed by a series of peaks at $m/z = 154$ (64%), 126 (73%), 98 (39%), 83 (11%), and 63 (100%); the mode of fragmentation of the ligand was compared with the spectra of the complexes. Molecular

Table 6. Mass spectral data of **1–3**.

Complex number	MS, m/z (%)
HL	$[\text{C}_7\text{H}_5\text{ClO}_3]^+$ 172(54) ^a , $[\text{C}_7\text{H}_3\text{ClO}_2]^+$ 154(64), $[\text{C}_6\text{H}_3\text{ClO}]^+$ 126(73), $[\text{C}_5\text{H}_3\text{Cl}]^+$ 98(39), $[\text{C}_4\text{H}_3\text{O}_2]^+$ 83(11), $[\text{COCl}]^+$ 63(100)
1	$[\text{C}_{22}\text{H}_{26}\text{O}_6\text{SnCl}_2]^+$ 576(n.o) ^a , $[\text{C}_{22}\text{H}_{27}\text{Cl}_2\text{O}_6\text{Sn}]^+$ 577(11), $[\text{C}_{15}\text{H}_{21}\text{ClO}_3\text{Sn}]^+$ 403(26), $[\text{C}_7\text{H}_4\text{ClO}_3\text{Sn}]^+$ 290(46), $[\text{C}_6\text{H}_3\text{ClO}_3\text{Sn}]^+$ 245(64), $[\text{C}_4\text{H}_9\text{Sn}]^+$ 176(10), $[\text{C}_7\text{H}_3\text{ClO}_2]^+$ 154 (53), $[\text{Sn}]^+$ 120(28), $[\text{C}_6\text{H}_4]^+$ 76(2), $[\text{C}_4\text{H}_9]^+$ 57(100), $[\text{C}_4\text{H}_2]^+$ 50(8)
2	$[\text{C}_{15}\text{H}_{22}\text{O}_3\text{SnCl}_2]^+$ 440(n.o) ^a , $[\text{C}_{15}\text{H}_{21}\text{ClO}_3\text{Sn}]^+$ 403(4), $[\text{C}_7\text{H}_6\text{ClO}_3\text{Sn}]^+$ 292(11), $[\text{C}_7\text{H}_4\text{ClO}_3\text{Sn}]^+$ 290(38), $[\text{C}_6\text{H}_4\text{ClO}_3\text{Sn}]^+$ 246(43), $[\text{C}_6\text{H}_4\text{OSn}]^+$ 211(6), $[\text{C}_4\text{H}_9\text{Sn}]^+$ 176(4), $[\text{C}_7\text{H}_3\text{ClO}_3]^+$ 172(39), $[\text{C}_7\text{H}_3\text{ClO}_2]^+$ 154(100), $[\text{C}_6\text{H}_3\text{ClO}]^+$ 126(71), $[\text{Sn}]^+$ 120(1), $[\text{C}_5\text{H}_3\text{Cl}]^+$ 98(18), $[\text{C}_4\text{H}_9]^+$ 57(80)
3	$[\text{C}_{10}\text{H}_{13}\text{O}_3\text{SnCl}]^+$ 335(n.o) ^a , $[\text{C}_3\text{H}_3\text{O}_2\text{Sn}]^+$ 190(1), $[\text{C}_7\text{H}_5\text{ClO}_3]^+$ 172(75), $[\text{C}_7\text{H}_3\text{ClO}_2]^+$ 154 (23), $[\text{C}_6\text{H}_5\text{ClO}]^+$ 128(42), $[\text{C}_6\text{H}_3\text{ClO}]^+$ 126(82), $[\text{C}_5\text{H}_3\text{Cl}]^+$ 98(25), $[\text{C}_5\text{H}_3]^+$ 63(100), $[\text{Sn}]^+$ 120(30)

^aMolecular ion peak (M^+); n.o. = not observed.

ion peak was not observed for **1–3**; the data thus support the earlier reports that in the mass spectra of the organometallic compounds with [O, O] donor ligands, the molecular ion peak $[M + \bullet]$ is generally not observed or is of very low intensity [34]. However, a prominent $M + 1$ ion peak at m/z 577(11%) appeared for **1**; the parent molecule proceeds through various steps and finally forms the Sn at $m/z = 120$ (28%) and C_4H_2 ($m/z = 50$ (8%)) cations as end products. In **3**, the peak at $m/z = 190$ (1%) for $[C_3H_3O_2Sn]^+$ fragment appears due to simultaneous loss of the three methyl groups and decomposition of phenyl group of the ligand or the primary fragmentation expels the whole organotin fraction from the complex to give a signal for **HL**, $[C_7H_5ClO_3]^+$ with $m/z = 172$ (75%).

3.5. X-ray crystallography

Single-crystal XRD study of **1** verifies the coordination of 5-chlorosalicylic acid with dibutyltin(IV) as depicted in figure 2; there are four molecules of the complex in each unit cell (figure 2). The packing diagram (figure 3) represents a structure completely different from a reported hexameric cyclic structure of a similar dibutyltin(IV) derivative of 3,5-di-isopropyl salicylic acid (DIPSA), where both the carboxylate and phenoxide terminals of DIPSA bind to tin through chelating and bridging coordination [17]. There are also reports of a tetrameric ladder-shaped stannoxane, $[\{nBu_2Sn(DTBSA)\}_2O]_2$ (where DTBSA = 3,5-di-tert-butyl salicylate ion), in which a central cyclic four-membered Sn_2O_2 core is linked to two terminal nBu_2Sn entities through μ_3-O ; the coordination geometry around each tin was best described as distorted trigonal bipyramidal [35]. However, in our present investigation, on **1**, there are discrete molecular units with a six-coordinate geometry and the two ligand units connected to Sn(IV) in a *trans* configuration. The introduction of a chloro-substituent on salicylic acid increases the electron density through

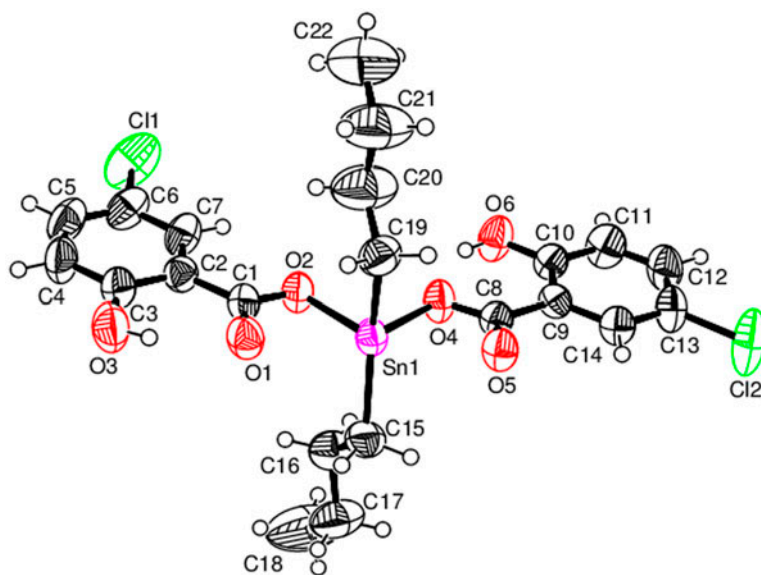


Figure 2. An ORTEP diagram of **1**. The thermal ellipsoids are drawn at 50% probability. The hydrogens are drawn as small circles of arbitrary level.

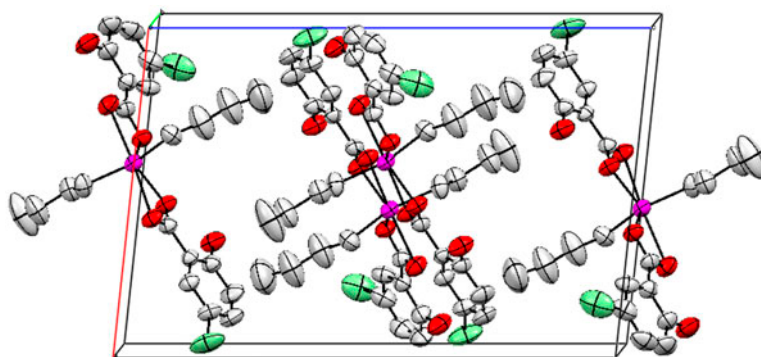


Figure 3. Packing diagram of **1** approximately viewed down the *b* axis. The hydrogens are omitted for clarity.

electron-donating resonance effect at phenolic -OH and thus renders difficulty in its deprotonation. So only carboxylate is deprotonated and undergoes complexation with Sn (IV) in an asymmetric bidentate mode. However, the ortho hydroxy group of chlorosalicylic acid develops intramolecular hydrogen bonding with nearby carbonyl oxygen [$\text{O1}\cdots\text{H3} = 1.895 \text{ \AA}$, $\text{O4}\cdots\text{H6} = 1.896 \text{ \AA}$; $\text{O3-H3-O1} = 144.9^\circ$, $\text{O4-H6-O6} = 145.5^\circ$] (figure 1). Such bonding was also documented in many organotin(IV) salicylates [27]. As **1** also contains phenolic functional group, this compound is a useful starting material for further reactions at -OH to build multimetallic systems by exploiting the highly acidic nature of the phenolic protons [35]. The four carboxylate oxygens from two ligand units lie in planar positions. Each carboxylate is bonded with the metal in an isobidentate mode with two shorter tin-oxygen bonds (Sn1-O1 , Sn1-O5) and two longer tin-oxygen bonds (Sn1-O2 and Sn1-O4), asymmetrically. The longer Sn-O distances ($\text{Sn1-O1} = 2.50 \text{ \AA}$ and $\text{Sn1-O5} = 2.53 \text{ \AA}$) are significantly less than the sum of the van der Waal's radii (3.68 \AA) [36]. The observed Sn1-O1 and Sn1-O5 bond lengths (2.50 and 2.53 \AA) are almost the same as those (2.48 and 2.53 \AA) observed for similar skew-trapezoidal bipyramid complexes reported earlier [11]. The asymmetric coordination mode of carboxylate was further confirmed by unequal C-O bond distances; $\text{O1-C1} = 1.256(6) \text{ \AA}$, $\text{O2-C1} = 1.279(5) \text{ \AA}$ and $\text{O4-C8} = 1.290(5) \text{ \AA}$, $\text{O5-C8} = 1.231(5) \text{ \AA}$. The two butyl groups attached to Sn atom occupy axial position with C19-Sn-C15 angle $152.2(3)^\circ$. As the four oxygens from the two chelating carboxylate ligands lie in the basal plane and two butyl groups are in distorted axial positions, thus **1** is the skew-trapezoidal or distorted octahedral geometry around tin [11]. Important crystal data and structure refinement parameters for **1** are given in table 7. Selected bond angles and lengths are given in table 8.

3.6. DNA interaction study

UV-visible absorption spectroscopy is the simplest technique for studying both the stability of DNA and its interaction with small molecules [37]. For the newly synthesized complexes, DNA binding parameters were evaluated by electronic absorption spectroscopy. The mode of interaction of metal with DNA was determined by comparison with absorbance and shifts in the wavelength range of $250\text{--}400 \text{ cm}^{-1}$ with and without SS-DNA (salmon sperm). The spectra have been recorded at different DNA concentrations by keeping concentration of the complexes constant. A single band appeared in absorption spectra at

Table 7. Crystal data and structure refinement parameters of **1**.

Chemical formula	C ₂₂ H ₂₆ Cl ₂ O ₆ Sn
Formula mass (g mol ⁻¹)	576.02
Crystal system	Monoclinic
Space group	<i>P</i> 2 ₁ / <i>c</i>
<i>a</i> (Å)	12.6055(8)
<i>b</i> (Å)	10.3491(7)
<i>c</i> (Å)	19.0644(13)
α (°)	90
β (°)	96.271(4)
γ (°)	90
Volume (Å ³)	2472.2(3)
<i>Z</i>	4
Temperature (K)	296(2)
Density (calculated) (g cm ⁻³)	1.548
Absorption coefficient (mm ⁻¹)	1.283
<i>F</i> ₍₀₀₀₎	1160.0
Radiation (Å) (Mo K α)	0.71073
Crystal size (mm ³)	0.3 × 0.2 × 0.18
Index ranges	-15 ≤ <i>h</i> ≤ 15, -10 ≤ <i>k</i> ≤ 12, -23 ≤ <i>l</i> ≤ 23
θ (°) min max	1.625–26.00
Total reflections	4849
Data/restraints/parameters	4849/0/284
<i>R</i> _{all} , <i>R</i> _{gt}	0.0734, 0.0399
WR _{ref} , WR _{gt}	0.1041, 0.0866
Goodness-of-fit	1.030

Table 8. Selected bond lengths (Å) and angles (°) for **1**.

C1–C2	1.473(6)	C15–Sn1	2.107(5)
C1–O1	1.256(6)	C19–Sn1	2.095(5)
C1–O2	1.279(5)	O1–Sn1	2.500(3)
C8–C9	1.477(6)	O2–Sn1	2.139(3)
C8–O4	1.290(5)	O4–Sn1	2.156(3)
C8–O5	1.231(5)	O5–Sn1	2.530(3)
C15–Sn1–O1	89.27(17)	O1–C1–O2	119.2(4)
C15–Sn1–O2	102.57(16)	O2–C1–C2	119.2(4)
C15–Sn1–O4	100.65(18)	C3–C2–C1	120.2(5)
C15–Sn1–O5	88.34(17)	C7–C2–C1	120.3(4)
C19–Sn1–C15	152.2(2)	C7–C2–C3	119.5(4)
C19–Sn1–O1	86.94(17)	O4–C8–C9	118.3(4)
C19–Sn1–O2	97.87(17)	O5–C8–C9	122.3(4)
C19–Sn1–O4	99.99(18)	O5–C8–O4	119.4(4)
C19–Sn1–O5	88.62(16)	C10–C9–C8	122.6(4)
O1–Sn1–O5	165.69(10)	C10–C9–C14	119.0(4)
O2–Sn1–O1	55.57(11)	C14–C9–C8	118.4(4)
O2–Sn1–O4	84.04(11)	C1–O1–Sn1	84.4(3)
O2–Sn1–O5	138.64(10)	C1–O2–Sn1	100.6(3)
O4–Sn1–O1	139.61(11)	C8–O4–Sn1	101.0(3)
O4–Sn1–O5	54.64(10)	C8–O5–Sn1	85.0(3)
O1–C1–C2	121.6(4)		

313.0 nm (**1**), 313.5 nm (**2**), and 313.5 nm (**5**). The UV spectra (figure 4) showed significant hypsochromic effect. Generally, hypsochromism and redshift are associated with intercalative binding of the complex to the double helix of DNA due to strong intercalation

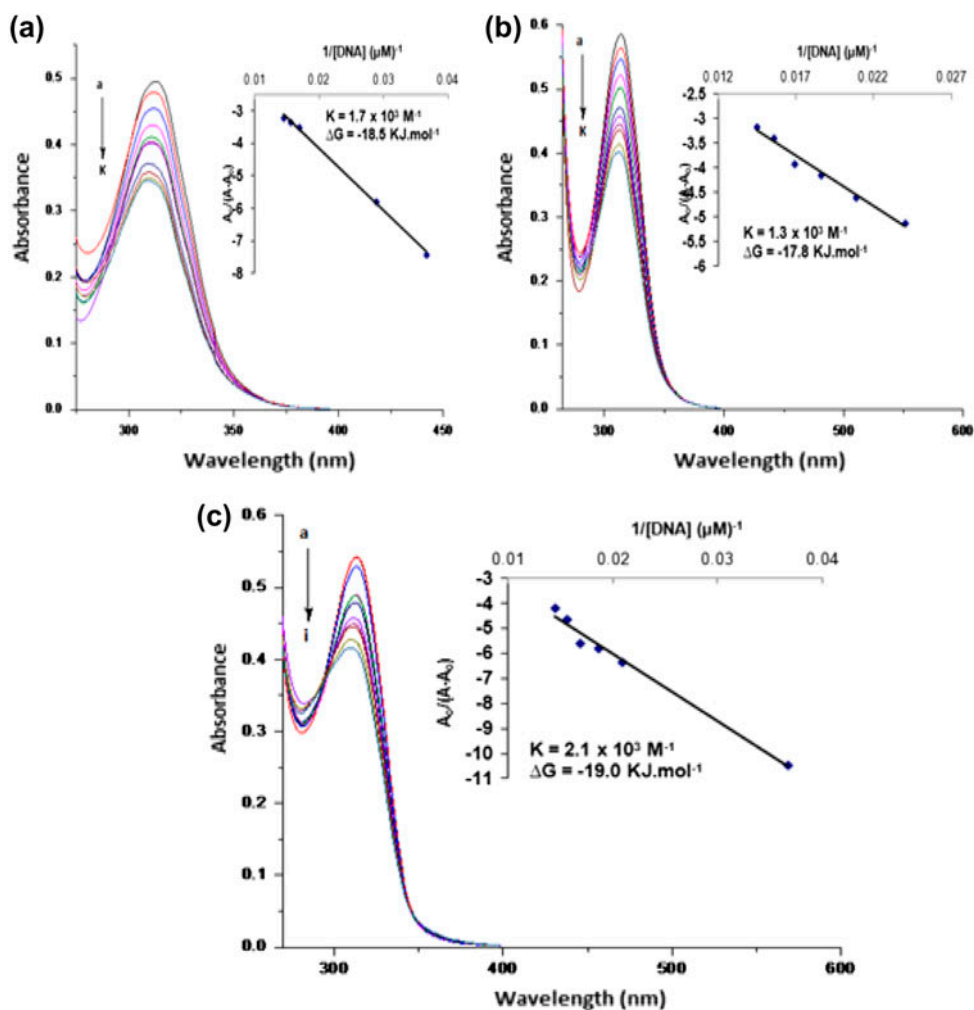


Figure 4. Absorption spectra of 2 mM of **1** (a), **2** (b), and **5** (c) in the absence (a) and presence of 10 μM (b), 19 μM (c), 27 μM (d), 35 μM (e), 42 μM (f), 48 μM (g), 54 μM (h), 59 μM (i), 64 μM (j), and 69 μM (k) DNA. The arrow direction indicates increasing concentrations of DNA. Inside graph is the plot of $A_0/(A - A_0)$ vs. $1/[\text{DNA}]$ for the determination of binding constant and Gibb's free energy of complex-DNA adduct.

between the complex and the base pairs of DNA. The extent of hypsochromism is commonly consistent with the strength of the intercalative interaction [38].

After 24 h, the spectrum was again taken, with the same results which confirmed the stability of drug-DNA complex. The intrinsic binding constants K for the DNA active complexes were calculated to compare binding strengths of ligand-DNA and complex-DNA using the Benesi–Hildebrand equation [39]:

$$\frac{A_0}{A - A_0} = \frac{\varepsilon_G}{\varepsilon_{\text{H-G}} - \varepsilon_0} + \frac{\varepsilon_G}{\varepsilon_{\text{H-G}} - \varepsilon_G} \times \frac{1}{K[\text{DNA}]}$$

where K = binding constant; A_0 = absorbance coefficient of drug-DNA complex. The association constants were obtained from the intercept-to-slope ratios of $A_0/(A - A_0)$ vs. $1/[DNA]$ plots. The binding constants were $1.7 \times 10^3 \text{ M}^{-1}$ (**1**), $1.3 \times 10^3 \text{ M}^{-1}$ (**2**), and $2.1 \times 10^3 \text{ M}^{-1}$ (**5**).

The DNA binding of the complexes was attributed to the presence of phenyl moieties as the presence of a phenyl group facilitates the interaction with double stranded DNA [40, 41]. That is the reason that **5** having the phenyl moieties in the ligand as well as in the organotin(IV) skeleton exhibited the highest binding with SS-DNA. The Gibb's free energies (ΔG) were determined using the following equation:

$$\Delta G = -RT \ln K$$

where R is general gas constant ($8.314 \text{ J K}^{-1} \text{ mol}^{-1}$) and T is the temperature (298 K). The Gibb's free energies were -18.5 (**1**), -17.8 (**2**), and -19.0 (**5**). The negative values suggest that the interaction of the compounds with DNA is a spontaneous process.

3.7. Antimicrobial activities

The ligand and complexes were screened to check their *in vitro* response against various bacterial strains (*E. coli*, *B. subtilis*, *S. aureus*, and *P. multocida*) and fungal strains (*A. alternata*, *G. lucidum*, *P. notatum*, *T. harzianum*, and *A. niger*). The activity was carried out by disk diffusion method [21], followed by measurement of MIC [23]. Streptomycin and fluconazole were used as the positive control for antibacterial and antifungal screening tests, respectively. The wells exhibiting MICs were noted visually, while the zones of inhibition of disks were measured in millimeters. The data are given in tables 9–12.

The literature [16, 42] shows that organotin(IV) complexes are biologically active with a few exceptions. The investigated organotin(IV) complexes possessed significantly higher antimicrobial activity toward the tested organisms as compared to **HL** [43]; thus, the growth inhibitory effects of **1–5** were greater than that of **HL** for bacterial as well as fungal strains. This increased activity of organotin(IV) carboxylates may be due to the coordination and polarity of tin(IV) with oxygens of the ligand [44]. The biological activities are varied according to the substitution pattern at tin [43]. The antibacterial activities (table 9) of dibutyltin(IV) complexes **1**, **2**, and triphenyltin(IV) derivative **5** were somewhat less than the

Table 9. Antibacterial activity data^a of **1–5**.

Complex number	Bacterial inhibition zone (mm)			
	<i>E. coli</i>	<i>B. subtilis</i>	<i>S. aureus</i>	<i>P. multocida</i>
HL	0	0	0	0
1	22 ^b ± 0.21	22 ^{bc} ± 0.24	25 ^{ab} ± 0.13	25 ^{bc} ± 0.26
2	22 ^b ± 0.15	25 ^{ab} ± 0.12	28 ^{ab} ± 0.23	28 ^{bc} ± 0.21
3	13 ^c ± 0.14	16 ^c ± 0.22	16 ^c ± 0.21	12 ^c ± 0.07
4	30 ^a ± 0.21	31 ^a ± 0.18	30 ^{ab} ± 0.14	70 ^a ± 0.37
5	19 ^{bc} ± 0.11	22 ^{bc} ± 0.19	23 ^b ± 0.12	18 ^{bc} ± 0.15
Streptomycin	30 ^a ± 0.17	31 ^a ± 0.28	31 ^a ± 0.31	29 ^{bc} ± 0.28

^aData are expressed as the mean ± standard deviation of samples analyzed individually in triplicate at $p < 0.1$; values having same letters in superscripts of the same column do not differ significantly; 0 = no activity, 5–10 = activity present, 11–25 = moderate activity, 26–40 = strong activity.

^bModerate activity.

^cLowest activity.

Table 10. Antifungal activity data^a of 1–5.

Complex number	Fungal inhibition zone (mm)				
	<i>A. alternata</i>	<i>G. lucidum</i>	<i>P. notatum</i>	<i>T. harzianum</i>	<i>A. niger</i>
HL	20 ^{bc} ± 0.17	16 ^c ± 0.11	0	0	20 ^{bc} ± 0.19
1	21 ^{bc} ± 0.16	21 ^{bc} ± 0.09	26 ^{bc} ± 0.16	21 ^c ± 0.19	30 ^{ab} ± 0.21
2	18 ^c ± 0.19	20 ^{bc} ± 0.12	21 ^{bc} ± 0.14	0	27 ^{bc} ± 0.16
3	18 ^c ± 0.11	18 ^{bc} ± 0.14	18 ^c ± 0.12	0	19 ^c ± 0.17
4	31 ^{ab} ± 0.21	30 ^{ab} ± 0.12	45 ^a ± 0.29	29 ^a ± 0.13	30 ^{ab} ± 0.11
5	21 ^{bc} ± 0.13	0	28 ^{bc} ± 0.22	22 ^{bc} ± 0.14	23 ^{bc} ± 0.14
Fluconazole	38 ^a ± 0.29	41 ^a ± 0.21	45 ^a ± 0.31	0	37 ^a ± 0.23

^aData are expressed as the mean ± standard deviation of samples analyzed individually in triplicate at $p < 0.1$; values having same letters in superscripts of the same column do not differ significantly; 0 = no activity, 5–10 = activity present, 11–25 = moderate activity, 26–40 = strong activity.

^bModerate activity.

^cLowest activity.

Table 11. MIC (bacterial) data of 1–5.

Complex number	Minimum inhibitory concentration ($\mu\text{g mL}^{-1}$)			
	<i>E. coli</i>	<i>B. subtilis</i>	<i>S. aureus</i>	<i>P. multocida</i>
HL	–	–	–	–
1	39	2.4	148	148
2	78	78	148	78
3	312	148	78	148
4	5	10	39	10
5	148	19	78	148
Streptomycin	1	2	78	39

standard drug (ampicillin). The trimethyltin(IV) derivative **3** exhibits antibacterial activity less than other synthesized organotin(IV) derivatives; the presence of methyl group enhances the lipophilic character of the ligand, but decreases the antimicrobial activity as reported earlier [45]. The triorganotin(IV) derivative **4** exhibited a higher inhibitory effect than its di-analogs **1** and **2** which may be due to greater lipophilicity and permeability through the cell membrane [46]. Moreover, the tributyltin(IV) derivative **4** showed higher antibacterial biopotency against the tested bacterial strains and its activity was either very close (against *S. aureus*, *E. coli*, or *B. subtilis*) to or even higher (against *P. multocida*) compared to streptomycin. Complex **4** exhibits highest antifungal potential, while **3** showed

Table 12. MIC (fungal) data of 1–5.

Complex number	Minimum inhibitory concentration ($\mu\text{g mL}^{-1}$)				
	<i>A. alternata</i>	<i>G. lucidum</i>	<i>P. notatum</i>	<i>T. harzianum</i>	<i>A. niger</i>
HL	–	–	–	6	–
1	208	104	104	6	6
2	416	104	52	6	13
3	208	104	208	13	52
4	6	1	13	1	13
5	208	104	104	52	13
Fluconazole	26	26	>0.4	416	–

Table 13. Hemolytic activity data of 1–5.

Complex number	HL	1	2	3
% Hemolysis	6.94 ± 0.03	34.39 ± 0.02	7.16 ± 0.03	6.34 ± 0.03
Complex number	4	5	Triton-X 100	PBS
% Hemolysis	10.23 ± 0.05	32.20 ± 0.03	99.53 ± 0.00	0.00 ± 0.00

least antifungal action (table 10) among the synthesized complexes. The results obtained from MIC (tables 11 and 12) also verify the high biopotency of **4** against all microbes (fungi and bacteria). MIC values of the complexes reveal strong differences in activities due to the nature of substituent present in Sn [41].

3.8. Hemolytic activity

The *in vitro* hemolytic bioassay of 1–5 was carried out with human red blood cells, and the average lysis was observed with respect to the Triton-X 100 as positive control (100% lysis) and PBS as negative control (0% lysis). The results are given in table 13.

The lowest activity (6.34%) was found for the trimethyltin(IV) derivative **3** and the highest value (34.39%) was recorded for **1**. The complexes displayed their hemolytic activities higher than **HL**. However, it is worth mentioning that 1–5 exhibited hemolytic activities which were lower as compared to Triton-X 100 and higher than PBS. Complex **4** which displayed excellent biopotency against fungal as well as bacterial strains showed very little hemolytic effects (10.23% lysis), thus almost enabling its possible safe use as an antibiotic drug.

4. Conclusion

FTIR data of 1–5 indicated bidentate chelating carboxylate and non-involvement of phenolic oxygen of the ligand in coordination with Sn(IV). There is intramolecular hydrogen bonding between ortho hydroxyl proton and carbonyl oxygen of tin bonded COO⁻ moieties. NMR data demonstrated six- and five-coordinate geometries in diorganotin and chlorodiorganotin/triorganotin carboxylates, respectively, in solution. The chloro-substituted salicylate ion causes an expansion of coordination number around tin(IV) as compared to simple organotin(IV) salicylates lacking the chloro-substituent. Each stannic ion appeared in the EIMS spectrum as a series of peaks close to each other due to isotopes and no molecular ion peak was observed. Single-crystal XRD of **1** showed skew-trapezoidal geometry with the ligand connected to Sn(IV) in a *trans* configuration. Complexes **1**, **2**, and **5** exhibited hypsochromic effect and intercalating mode of binding with SS-DNA. The increased antimicrobial activities of organotin(IV) carboxylates as compared to the parent ligand are due to the coordination and polarity of tin(IV) with oxygens of the ligand. The biological potential varied according to the substitution pattern at tin(IV) and the triorganotin(IV) derivatives exhibited a higher inhibitory effect than their di-analogs. Complex **4** was the most potent inhibitor of bacteria and fungi, with minor hemolytic activity.

Supplementary material

Crystallographic data for **1** has been deposited with the Cambridge Crystallographic Data Center, CCDC No. 1024920. Copies of this information may be obtained free of charge from the Director, CCDC12 Union Road, Cambridge, CBZ IEZ, UK (Fax: +44 1223 336 033; Email: deposit@ccdc.cam.ac.uk or [www: http://www.ccdc.cam.ac.uk](http://www.ccdc.cam.ac.uk)).

Acknowledgment

SH thanks the HEC, Islamabad, Pakistan, for financial support under the PhD Fellowship Scheme Batch-IV (PIN Code: 074-3160-Ps4-362).

Disclosure statement

No potential conflict of interest was reported by the authors.

References

- [1] A. Ross. *Ann. N.Y. Acad. Sci.*, **125**, 107 (1965).
- [2] P. Fierens, G.V.D. Vandendunghen, W. Segers, R.V. van Elsuwe. *React. Kinet. Catal. Lett.*, **8**, 179 (1978).
- [3] S. Karpel. *Tin Uses*, **149**, 1 (1986).
- [4] F.W. van Der Weij. *Macromol. Chem.*, **181**, 2541 (1980).
- [5] A.A. Mahmoud, A.F. Shaaban, M.M. Azab, N.N. Messiha. *Eur. Polym. J.*, **28**, 555 (1992).
- [6] R. Gachter, H. Muller. *Plastics Additives Handbook*, Hanser Publisher, Munich (1990).
- [7] M. Tariq, N. Muhammad, M. Sirajuddin, S. Ali, N.A. Shah, N. Khalid, M.N. Tahir, M.R. Khan. *J. Organomet. Chem.*, **723**, 79 (2013).
- [8] L. Pellerito, L. Nagy. *Coord. Chem. Rev.*, **224**, 111 (2002).
- [9] M.I. Khan, M.K. Kaleem Baloch, M. Ashfaq. *J. Organomet. Chem.*, **689**, 3370 (2004).
- [10] X. Shang, X. Meng, E.C.B.A. Alegria, Q. Li, M.F.C. Guedes da Silva, M.L. Kuznetsov, A.J.L. Pombeiro. *Inorg. Chem.*, **50**, 8158 (2011).
- [11] A.G. Davies, P.J. Smith. *Adv. Inorg. Chem. Radiochem.*, **23**, 1 (1980).
- [12] S.M. Abbas, S. Ali, S.T. Hussain, S. Shahzadi. *J. Coord. Chem.*, **66**, 2217 (2013).
- [13] E.R.T. Tiekink. *Appl. Organomet. Chem.*, **5**, 1 (1991).
- [14] S. Hussain, S. Ali, S. Shahzadi, C. Rizzoli. *Phosphorus, Sulfur Silicon Relat. Elem.*, **188**, 812 (2013).
- [15] S. Hussain, S. Ali, S. Shahzadi, S.K. Sharma, K. Qanungo, I.H. Bukhari. *J. Coord. Chem.*, **65**, 278 (2012).
- [16] S. Shahzadi, K. Shahid, S. Ali. *J. Coord. Chem.*, **60**, 2637 (2007).
- [17] G. Prabusankar, R. Murugavel. *Organometallics*, **23**, 5644 (2004).
- [18] W.L.F. Armarego, C.L.L. Chai. *Purification of Laboratory Chemicals*, 5th Edn, Butterworth Heinemann, London (2003).
- [19] Y. Zhang, X. Wang, L. Ding. *Nucleos. Nucleot. Nucl. Acids*, **30**, 49 (2011).
- [20] C.V. Sastri, D. Eswaremoorthy, L. Giribabu, B.G. Maiya. *J. Inorg. Biochem.*, **94**, 138 (2003).
- [21] CLSI (The Clinical Laboratory Standards Institute). *J. Clin. Microbiol.*, **45**, 2758 (2007).
- [22] G. Huang, S.J. Moore, J. Jiaxin, D. Dehui. *Food Sci. Technol.*, **11**, 25 (2001).
- [23] S.D. Sarker, L. Nahar, Y. Kumarasamy. *Methods*, **42**, 321 (2007).
- [24] P. Sharma, J.D. Sharma. *J. Ethnopharmacol.*, **74**, 239 (2001).
- [25] P.J. Smith, R.O. Day, V. Chandrasekhar, J.M. Holmes, R.R. Holmes. *Inorg. Chem.*, **25**, 2495 (1986).
- [26] G. Eng, X. Song, A. Zapata, A.C. de Dios, L. Casabianca, R.D. Pike. *J. Organomet. Chem.*, **692**, 1398 (2007).
- [27] J.F. Vollano, R.O. Day, D.N. Rau, V. Chandrasekhar, R.R. Holmes. *Inorg. Chem.*, **23**, 3153 (1984).
- [28] M. Rizwan, S. Ali, S. Shahzadi, S.K. Sharma, K. Qanungo, M. Shahid, S. Mahmood. *J. Coord. Chem.*, **67**, 341 (2014).
- [29] T.P. Lockhart, W.F. Manders, E.M. Holt. *J. Am. Chem. Soc.*, **108**, 6611 (1986).
- [30] R.R. Holmes, R.O. Day, V. Chandrasekhar, J.F. Vollano, J.M. Holmes. *Inorg. Chem.*, **25**, 2490 (1986).

- [31] J. Holecek, K. Handlir, M. Nadvornik, A. Lycka. *Z. Chem.*, **30**, 265 (1990).
- [32] A.G. Davis, P.J. Smith. In *Comprehensive Organometallic Chemistry*, G. Wilkinson, F.G.A. Stone, E.W. Abel (Eds.), p. 967, Pergamon Press, Oxford (1982).
- [33] S. Shahzadi, K. Shahid, S. Ali, M. Mazhar, A. Badshah, E. Ahmed, A. Malik. *Turk. J. Chem.*, **29**, 273 (2005).
- [34] M. Danish, S. Ali, M. Mazhar. *Heteroatom Chem.*, **7**, 223 (1996).
- [35] R. Murugavel, N. Gogoi. *J. Organomet. Chem.*, **693**, 3111 (2008).
- [36] E.R.T. Tiekink. *Trends Organomet. Chem.*, **1**, 71 (1994).
- [37] F. Javed, S. Ali, M.W. Shah, K.S. Munawar, S. Shahzadi. *J. Coord. Chem.*, **67**, 2795 (2014).
- [38] S.A. Tysoe, R.J. Morgan, A.D. Baker, T.C. Streckas. *J. Phys. Chem.*, **97**, 1707 (1993).
- [39] M.S. Ahmad, M. Hussain, M. Hanif, S. Ali, B. Mirza. *Molecules*, **12**, 2348 (2007).
- [40] M. Tariq, S. Ali, N. Muhammad, N.A. Shah, M. Sirajuddin, M.N. Tahir, N. Khalid, M.R. Khan. *J. Coord. Chem.*, **67**, 323 (2014).
- [41] S. Hussain, I.H. Bukhari, S. Ali, S. Shahzadi, M. Shahid, K.S. Munawar. *J. Coord. Chem.*, **68**, 662 (2015).
- [42] N. Sharma, V. Kumar, M. Kumari, A. Pathania, S.C. Chaudhry. *J. Coord. Chem.*, **63**, 3498 (2010).
- [43] S. Hussain, S. Ali, S. Shahzadi, S.K. Sharma, K. Qanungo, M. Shahid. *Bioinorg. Chem. Appl.*, **2014**, 1 (2014).
- [44] N. Singh, S. Gupta, G. Nath. *Cent. Nat. De La Rech. Sci., (CAT.INIST)*, **14**, 484 (2000).
- [45] A. Bacchi, M. Carcelli, P. Pelagatti, G. Pelizzi, M.C. Rodriguez-Arguelles, D. Rogolino, C. Solinas, F. Zani. *J. Inorg. Biochem.*, **99**, 397 (2005).
- [46] Y. Shi, B.Y. Zhang, R.F. Zhang, S.L. Zhang, C.L. Ma. *J. Coord. Chem.*, **65**, 4125 (2012).